Membrane Structure Drives Synchronization Patterns in Arrays of Diffusively Coupled Self-Oscillating Droplets

Membrane Structure Drives Synchronisation Patterns in Arrays of Diffusively Coupled Self-Oscillating Droplets

Marcello A. Budroni,[†,‡] Kristian Torbensen,[¶] Sandra Ristori,[§] Ali Abou-Hassan,[*,¶] and Federico Rossi[*,‖]

†*Nonlinear Physical Chemistry Unit, Faculté des Sciences, Université libre de Bruxelles (ULB), CP231, 1050 Brussels, Belgium*

‡*Present address: Department of Chemistry and Pharmacy, University of Sassari, Via Vienna 2, 07100 Sassari, Italy*

¶*Sorbonne Université, CNRS, PHysico-chimie des Electrolytes, Nanosystémes InterfaciauX (PHENIX), F-75005 Paris, France*

§*Department of Chemistry & CSGI, University of Florence, Via della Lastruccia 3, 50019 Sesto Fiorentino, Firenze, Italy*

‖*Department of Physical Science, Earth and Environment, University of Siena, Pian dei Mantellini, 44 53100 Siena (SI), Italy*

E-mail: ali.abou_hassan@sorbonne-universite.fr; federico.rossi2@unisi.it

Abstract

Networks of diffusively coupled inorganic oscillators, confined in nano- and micro-compartments are effective to predict and understand the global dynamics of those systems where the diffusion of activatory or inhibitory signals regulates the communication among different individuals. By taking advantage of a microfluidic device,

we study the dynamics of arrays of diffusively-coupled Belousov-Zhabotinsky (BZ) oscillators encapsulated in water-in-oil single emulsions. New synchronization patterns are induced and controlled by modulating the structural and chemical properties of the phospholipid-based biomimetic membranes *via* the introduction of specific dopants that do not alter their basic backbone but modify the membrane lamellarity (and, in turn, their permeability) or interact chemically with the reaction intermediates. A transition from 2-period clusters showing 1:2 period-locking to 1-period antiphase synchronization is observed by decreasing the membrane lamellarity. An unsynchronized scenario is found when the dopant is able to interfere with chemical communication by reacting with the chemical messengers.

TOC Graphic

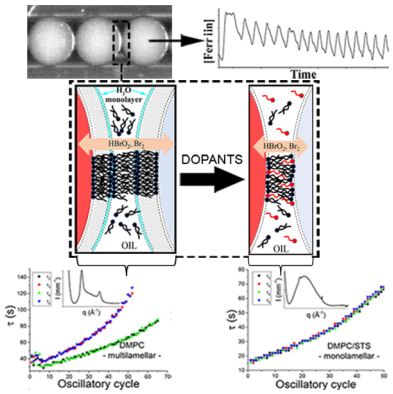

Communication through passive molecular diffusion is a ubiquitous strategy by which biological systems exchange signals and information for short- and long-range interactions. This mechanism operates over a wide spatial domain, ranging from nanometers (intracellular) to hundreds of micrometers (intercellular).[1,2] When coupled with autocatalysis, passive communication mechanism can bear the information from cell to cell over the macroscopic scale of meters as a reaction-diffusion wave.[3] Signal molecules generally can be divided into two major classes: activators, that promote specific process or deliver positive feedbacks (chemotaxis, quorum sensing) and inhibitors, that work in the opposite way.[4,5] Sometimes, a messenger molecule (e.g. Ca^{2+}) can act both as positive and negative feedback depending on its concentration amplitude and frequency in modulated oscillatory signals.[3,6]

The exchange of intercellular signals is particularly relevant when a coordinate and synchronous activity of many cells is required to express a physiological function, such as neural activity, cardiac contraction/expansion, calcium-signalling dynamics and quorum sensing, to name a few.[3,7–10] Although biological systems have developed a wealth of strategies for active communication of chemical signals, *e.g. via* microtubules, gap-junctions, etc., passive diffusion through cell membranes represent a viable mechanism to spread and receive signals without consuming metabolic energy and requiring communication *infrastructures.*[11]

In this context, diffusively coupled chemical oscillators, based on the Belousov-Zhabotinsky (BZ) reaction,[12,13] represent a reliable model for studying collective and emergent behaviours observed in cellular environment.[10] To mimic and understand such collective behaviour, the chemical oscillators can be encapsulated inside micro-compartments, throughout which passive diffusion is allowed, in order to recreate the cell confinement and intercellular communication. In addition, such compartments should be generated in a controllable manner to allow the multi-scale fine tuning of their characteristics, including chemical composition, the physico-chemical properties of the liquid/liquid interface and macroscopically their number and dimensions (size and polydispersity) as well as their spatial organisation. Microfluidics can offer unprecedented opportunities to finely tune such parameters. Consequently, follow-

ing the introduction of microfluidics,[14,15] it was established how the dispersion medium,[16] the balance between excitatory and inhibitory signals[17,18] and the network geometry,[19–21] select the global dynamics (in-phase and anti-phase oscillations, phase and period clusters, etc.) of oscillating droplets encapsulating the Belousov-Zhabotinsky (BZ) oscillating reaction in surfactant stabilised water-in-oil (w/o) simple emulsions. A specifically designed experimental configuration of coupled BZ oscillators[22] was also employed to test the Turing theory about the intercellular reaction-diffusion mechanisms at the basis of pattern selection in morphogenetic processes.[23–25]

By taking advantage of flow-focusing microfluidic techniques, we introduced the use of phospholipid-based membranes to explore the influence of a biomimetic bilayer on the global dynamics of coupled liposomes,[26] simple w/o in oil emulsions[27] and double w/o/w emulsions,[28] containing the BZ reaction. In-phase and out-of-phase oscillations were the most frequently observed dynamics, depending whether the activator ($HBrO_2$) or the inhibitor (Br_2) were the predominant coupling species, respectively. Moreover, it was shown that molecular communication among droplets could be chemically hindered by intercalating cholesterol (Chol) in the membrane, a scavenger for both Br_2 and for some radical species ($BrO_2^{\bullet}$), known to be precursors of $HBrO_2$. This particular mechanism can be considered a prototype for chemically-based (i.e. active) and diffusion-mediated communication.

The space (x) and time (t) scales of communication through passive diffusion depend upon the diffusivity (D) of the signal molecule ($x \propto \sqrt{Dt}$), and are also regulated by the permeability (P) of the messenger species through the cell membranes, being the latter tightly related to the chemo-physical properties of the signal molecules (size, polarity, hydrophilicity, etc.). In particular P directly depends on the membrane thickness (d) and on the partition coefficient (α) of the diffusive molecules between the inner and the outer phases of the cell, according to $P \propto \alpha D/d$. The chemical nature and the structure of the cell membrane is thus of paramount importance in modulating the signals and, therefore, the final dynamics of the cellular network.[29]

Here we show that by modulating the membrane packing properties, the relative permeability of excitatory and inhibitory messengers could be tuned to yield different macroscopic dynamical behaviours and select different synchronisation schemes in 1-dimensional arrays of w/o BZ micro-oscillators.

The BZ w/o microdrops were generated by the microfluidic device sketched in Figure 1[27,30] and stabilised with the phospholipid 1,2-dimyristoyl-*sn*-glycero-3-phosphocholine (DMPC); membranes were successively doped with different amphiphilic molecules in a percentage (20%) that did not alter their basic backbone but changed the bilayer properties (*i.e.* lamellarity, packing defects and surface charge) of the lipid shells. The final experimental configuration is presented in Figure 1. The collective dynamics of the oscillating drops was observed and recorded with a microscope mounted with a CCD camera. Space-time plots and time-series of each oscillating BZ drop were then reconstructed from the movie frames (experimental information are detailed in the Supporting Information, SI). Three dopants having the same hydrophobic 14-C tail of DMPC, but different polar heads, were employed, namely the neutral myristic acid (Myr-A), the positively charged tetradecyl-amine (TA) and the negatively charged tetradecyl sulfate (STS, sodium salt). The structure of the oil/water interface in simple DMPC-stabilised emulsion is quite complex, being the boundary layer $\sim$100 μm with phospholipids arranged either as L3 sponge phase or as polydisperse unilamellar vesicles in a mixed oil/water medium.[31] However, when droplets are brought close to each other, as in the 1-D array configuration, the contact area between membranes is expected to form a spatially extended bilayer that provides a diffusive pathway for the chemical communication among successive drops. Although DMPC tended to form multilamellar membranes, the addition of dopants decreased progressively the lamellarity following the order Myr-A, TA and STS, with DMPC/STS membranes being monolamellar.[30] By modifying the composition of the membranes and their tendency to self-assembly into multilamellar structures, we were able to change the diffusion path, select the chemical messengers effectively operational in the coupling mechanism, and tune the coupling strength.

The experimental dynamics were interpreted within a unique kinetic framework, based on the paradigmatic Field, Köros and Noyes (FKN) model[32,33] widely adopted for describing the BZ system (see more details in the SI). The model equations read

$$\begin{aligned}
\frac{dc_1^i}{dt} &= -k_1 c_1^i c_2^i + k_2 c_2^i - 2k_3 (c_1^i)^2 + k_4 c_1^i \frac{(c_0 - c_4^i)}{(c_0 - c_4^i + c_{min})} \\
&\quad -k_X (c_1^i - c_1^{i+1}) - k_X (c_1^i - c_1^{i-1}) - f(s, c_1^i, k_s^X) \qquad (1) \\
\frac{dc_2^i}{dt} &= -3k_1 c_1^i c_2^i - 2k_2 c_2^i - k_3 (c_1^i)^2 + k_6 c_3^i + k_9 c_4^i \qquad (2) \\
\frac{dc_3^i}{dt} &= 2k_1 c_1^i c_2^i + k_2^i c_2^i + k_3 (c_1^i)^2 - k_6 c_3^i \\
&\quad -k_W (c_4^i - c_4^{i+1}) - k_W (c_4^i - c_4^{i-1}) - g(s, c_3^i, k_s^W) \qquad (3) \\
\frac{dc_4^i}{dt} &= 2k_4 c_1^i \frac{(c_0 - c_4^i)}{(c_0 - c_4^i + c_{min})} - k_9 c_4^i \qquad (4) \\
\frac{ds}{dt} &= -f(s, c_1^i, k_s^X) - g(s, c_3^i, k_s^W)\,. \qquad (5)
\end{aligned}$$

Here $\{k_i\}$ is the set of rate constants with values reported in the SI, $c_1^i = [\mathrm{HBrO_2}]$ is the autocatalytic species (activator), $c_2^i = [\mathrm{Br^-}]$, $c_3^i = [\mathrm{Br_2}]$ is the inhibitor and $c_4^i = [\mathrm{Fe^{3+}}]$ is the oxidized form of the catalyst in the i–th oscillator. c_{min} is a small constant which avoids equations to diverge due to the autocatalytic term[34] and c_0 the catalyst total concentration. The concentration of the initial reactants $[\mathrm{H^+}]$, $[\mathrm{BrO_3^-}]$, [MA] and the brominated organic substrate [BrMA] are assumed to vary negligibly slow with respect to the time-scale of the oscillatory dynamics of the reaction intermediates, and are thus included as constant pseudo-parameters into the rate constants (*pool chemical approximation*).[35] We implemented this kinetic scheme in a point-wise array of BZ microoscillators, where each drop (consisting of the BZ core and the surrounding lipidic shell) communicates with the closest neighbours *via* mass transfer of those species able to cross the lipid layer, namely $\mathrm{HBrO_2}$ and $\mathrm{Br_2}$.[7] The corresponding coupling terms $k_X(c_1^i - c_1^j)$ and $k_W(c_3^i - c_3^j)$ describe the excitatory and the inhibitory coupling among successive oscillators i and j, respectively. The relative impor-

tance of the two possible coupling schemes is tuned by parameters k_X and k_W, respectively, both depending on the membrane permeability as $k_I = 3P_i/R \propto \alpha_i D_i/(dR)$, where R is the droplet radius. Indeed, increasing the lamellarity of the drops membrane increases the inter-drops distance, and, in turn, decreases the permeability. Accordingly, an increment of the droplet global curvature, that scales as $1/R$, would also yield a similar effect. Modifications induced by dopants to the local membrane curvature, on the contrary, have a negligible impact on k_I. Reliable values for the corresponding coupling parameters typically range between [10^{-4}–10^{-3}] s^{-1} for k_X and [10^{-3}–10^{-1}] s^{-1} for k_W.[27,28] Our parametric exploration spans this region and shows that the contribution of the excitatory coupling is negligible and the inhibitory coupling mainly drives the synchronization in this system. The general kinetic functions $f(s, c_1^i, k_s^X)$ and $g(s, c_3^i, k_s^W)$ include possible chemical interactions between the dopant of the DMPC lipid membrane, S (with concentration s), and the chemical messengers. Since Br_2 is the main chemical messanger, we only consider a reaction between S and the inhibitor, regulated by the constant rate k_s^W (i.e. $f(s, c_1^i, k_s^X)$=0).

Although the regimes obtained by varying the system parameters are robust, parametric conditions for their occurrence can slightly change with the number of the oscillators in the array. We thus standardize our numerical exploration to an array of 4 microoscillators, each with a different starting frequency obtained by using different initial concentrations of the main BZ reactants, taken from gaussian distributions centred on the experimental values.

STS/DMPC (Monolamellar membranes): Anti-phase synchronization. A typical *anti-phase* synchronization is obtained by doping the lipidic membranes with the negatively charged surfactant STS. This dopant was shown to minimize the lamellarity of single emulsions to monolamellar structures,[30] activating a direct transfer of the lipo-soluble inhibitor Br_2, which thus controls here the chemical communication. This scenario has been already discussed in a previous work[27] and an analogous synchronization scheme has been found with the BZ oscillator encapsulated in arrays of AOT-microemulsions.[14] Here we reinvestigated this configuration in the framework of the new kinetic model adopted and results are shown

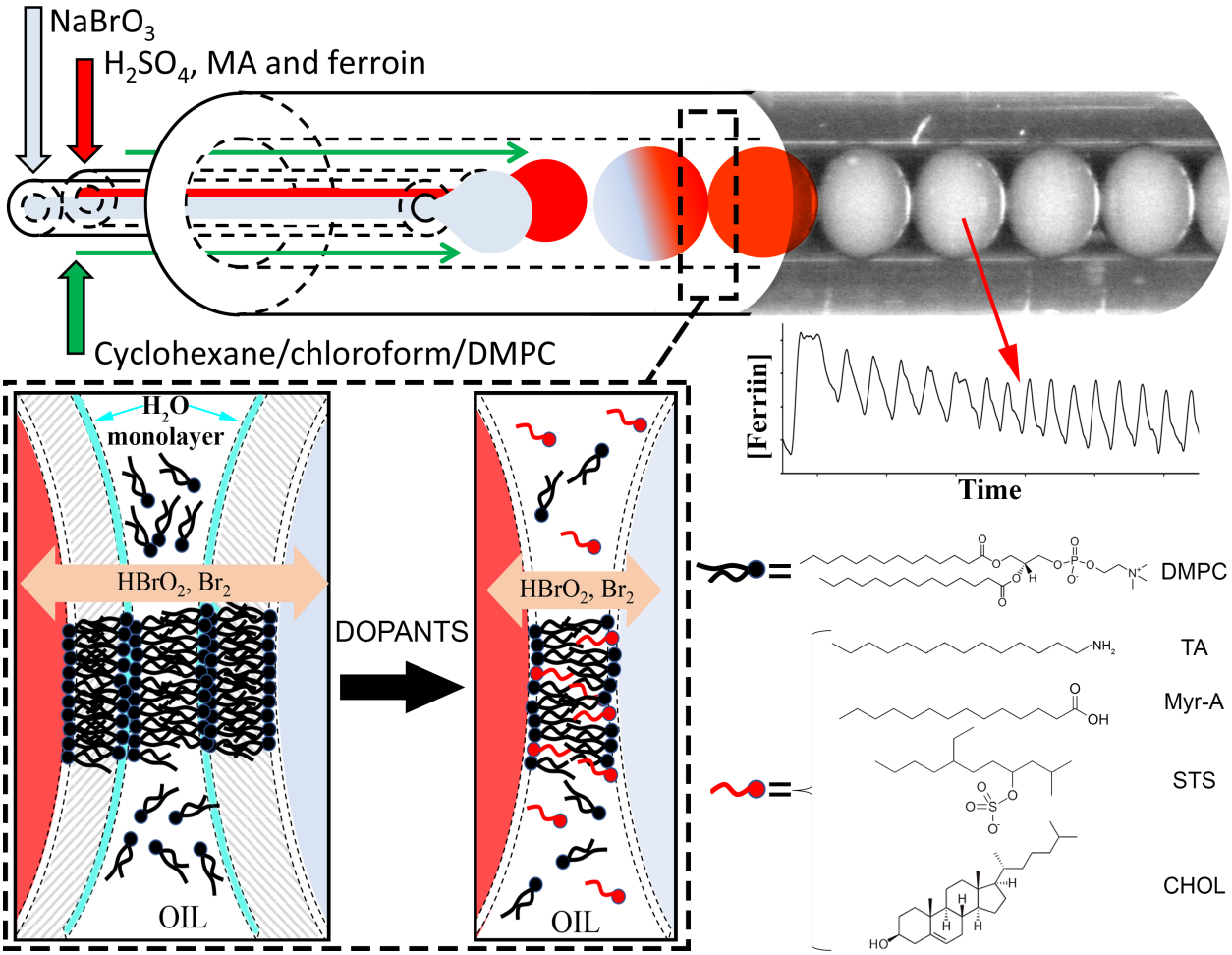

Figure 1: Sketch of the microfluidic device used to generate arrays of w/o simple emulsions. The sketch shows the coaxial flow of the BZ reactants prior to the drop formation. The resulting 1D array of BZ containing droplets are collected in a PTFE tube for monitoring. The bottom part represents the two extreme membrane's arrangements obtained with pure DMPC (multilamellar) and with DMPC + DOPANTS (monolamellar).

in the SI. In brief, defining each microoscillator phase as

$$\varphi_i(t) = \frac{2\pi\,(t - t_k)}{(t_{k+1} - t_k)} + 2k\pi \qquad t_k \le t \le t_{k+1}\ , \tag{6}$$

(where k is the peak label) alternate microoscillators tend to synchronize *in-phase* (with a vanishing small phase difference, $\Delta\varphi = \varphi_i - \varphi_j$), while adjacent oscillators present a phase lock close to π. All the microoscillators dynamically asymptotise to a unique period, τ'. We denote this scenario 1:1*:1:1*, where "*" indicates the π phase-shift among successive

oscillators.

DMPC (multilamellar membranes): Two-period clusters and 1:a:1:a period-locking. A second coupling scenario is obtained by using simple emulsions with pure DMPC multilamellar membranes.[30] Multilamellarity (and related effect on the diffusive path between drops through the organic medium) is expected to have a largest impact on lipo-soluble molecules like Br_2 thus reducing the inhibitory coupling. In the model this corresponds to decrease the importance of k_W. Numerical results in Figs. 2(g–h) favourably compare with the behaviours obtained experimentally, displayed in Figs. 2(a–d). We observe the emergence of two clusters of oscillation periods, τ' and τ''. Microoscillators with period τ' (O1 and O3) alternate with those characterised by period $\tau'' > \tau'$ (O2 and O4). This picture describes a *period-locking* synchronisation, tending to the period ratio 1 : 2 (see also SI). In the experiments, alternated microoscillators with same τ present a constant vanishing phase shift, while it stabilises to π in simulations. In both experimental and simulated dynamics, the phase difference $\Delta\varphi = \varphi_i - \varphi_j$ between adjacent oscillators (i, j) with general period-locking 1:a (where $a = \tau_j/\tau_i$) does not indicate any stationary correlation. However a relationship of the type $\varphi_i - a\varphi_j =$ constant (with $a \geq 1$ and tending to 2 in the course of the experiment) can be observed. Such synchronization pattern is quite unusual in 1-D arrays of diffusively coupled oscillators. In fact, BZ droplets oscillating with different periods were reported for simple emulsions separated by a fluorinated oil and having a low content of malonic acid[36] or for a system with a global negative feedback imposed from the external.[37] However, a clear 1:2:1:2 period-locking was never observed in the absence of external stimuli.

Myr-A/DMPC and TA/DMPC (Oligolamellar membranes): Two period clusters. An intermediate scenario was obtained when Myr-A or TA were used as membrane dopants. From a structural point of view, these two molecules markedly decrease the lamellarity of the lipids arrangement.[30] In both cases, the oscillating periods of alternate droplets in the array,

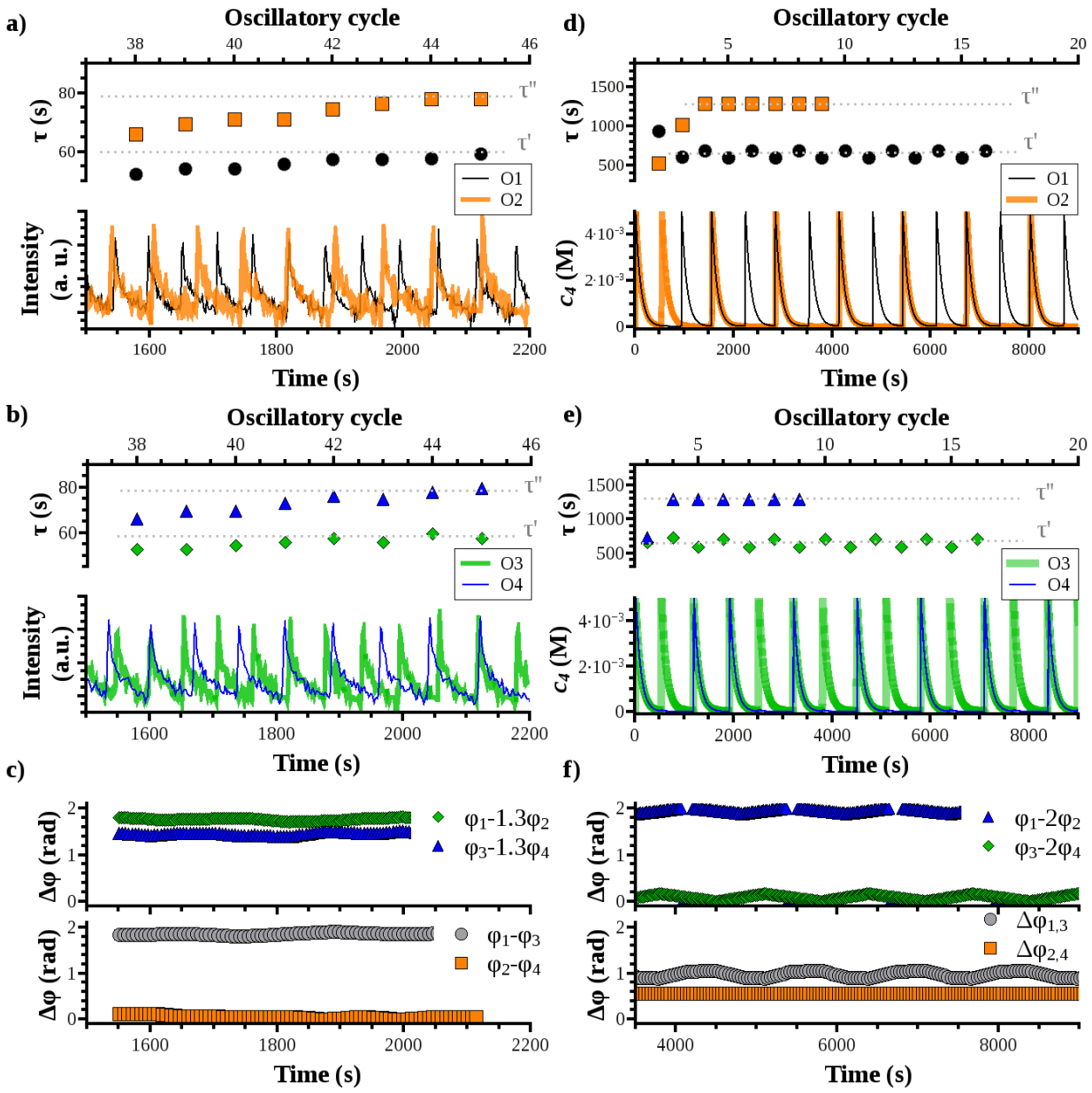

Figure 2: Experiments: a–b) Time series and profile of the oscillation period, τ, of adjacent pairs of BZ oscillators suspended in an oil phase containing 1% DMPC. The period analysis shows the presence of two populations of microoscillators with period $\tau' \in (50, 60)$ s (O1 and O3) and $\tau'' > \tau'$ ($\tau'' \in (70, 80)$ s, O2 and O4). Microoscillators progressively stabilize to a *1:2:1:2 period-locking* scenario (see also Fig. 4). c) The analysis of the phase difference, $\Delta\varphi$, indicates that if i and j are adjacent oscillators, a relation of the type $\varphi_i - a\varphi_j =$ constant (with $a = \tau_j/\tau_i$ tending to 2 in the course of the experiment) holds. Simulations: d–f) Time series describing the concentration of the oxidised form of the catalyst, c_4, τ and $\Delta\varphi$ of the corresponding scenario simulated by integrating model eqs. (1–4) with $k_X \leq 0.001$ s^{-1} and $k_W = 0.006$ s^{-1}, $k_9 = 0.3$[MA] s^{-1}. The other parameters are listed in the SI.

clustered in two different values, having a percentage difference in the range 10–20% (see Figure 4 in SI). Alternate droplets also oscillated in phase-lock regime, namely π for MYR-A and $\sim 0.5\pi$ for TA, highlighting a more pronounced inhibitory coupling for the neutral species MYR-A. As an example, Fig. 3 reports the experimental and simulated timeseries of 4 communicating droplets doped with TA. Note that all these synchronisation scenarios induced by a weak inhibitor exchange, are simulated not only by decreasing k_W, but also *via* a parallel increment of the kinetic constant k_9 (controlling the resetting step of the chemical clock, see SI). The retention of bromine in each oscillators, in fact, can increase the amount of local bromomalonic acid, which concentration is embedded in k_9 in the kinetic model.

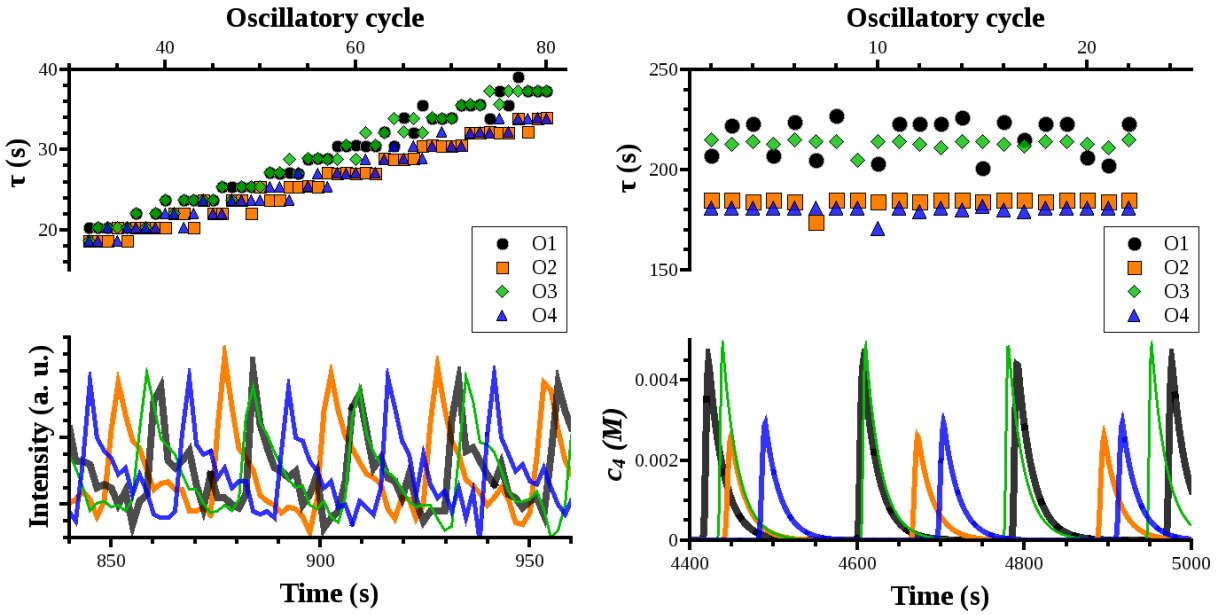

Figure 3: a) Experimental time series and profile of the oscillation period, τ, of BZ oscillators suspended in an oil phase containing 1% DMPC doped with TA. The period analysis shows the emergence of two populations of microoscillators with different period, $\tau'' > \tau'$, where alternate oscillators present coherent behaviour 1:1.2:1:1.2. b) Simulation of the corresponding scenario by integrating model eqs. (1–4) with $k_X \leq 0.001$ s^{-1}, $k_W = 0.003$ s^{-1}, $k_9 = 0.3$[MA] s^{-1}. The other parameters are listed in the SI.

Chol/DMPC (multilamellar membranes): No synchronisation. We finally discuss a situation in which a membrane dopant rather than affecting the structural properties of the membrane, can chemically interact with the messenger species, thus interfering with the drops coupling. As previously mentioned, when cholesterol was introduced in the lipid mem-

brane to serve as a Br_2 blocking agent, the inhibitory species (which dominates the chemical coupling) is prevented from driving any chemical communication among oscillators.[27] Here we reinvestigated this behaviour within the framework of the new model by including the interaction between Br_2 and a sequestrating dopant S, according to $Br_2 + S \xrightarrow{k_s} S - Br_2$, giving $g(c_3^i, s, k_s^W) = -k_s^W c_3^i\, s$ ($k_s^W \in [2000, 5000]$ $M^{-1}s^{-1}$).[33] Consistently with previous work, we found uncorrelated patterns of the oscillations among different microoscillators (see SI). The fact that suppressing the inhibitory coupling leads to uncoupled dynamics further confirm that the excitatory contribution is essentially negligible.

Table 1: Summary of collective behaviours obtained in arrays of BZ drops encapsulated in W/O doped single emulsions.

Membrane composition	**Lamellarity**	**Coupling scheme**	**Synchronization pattern**
DMPC + STS	Monolamellar	Strong inhibitory	*Anti-phase* 1:1*:1:1*
DMPC + TA (or Myr-A)	Oligolamellar	Weak inhibitory	Two-period clustering 1:1.2:1:1.2
DMPC	Multilamellar	Weak inhibitory	Two-period clustering *1:2:1:2 Period-locking*
DMPC + Chol	Multilamellar	No coupling	*Unsynchronised*

Table 1 summarises the characteristics of the control parameters of the different dynamical regimes found by modulating the chemical and structural properties of biomimetic membranes in arrays of coupled BZ microoscillators. The dependence of the synchronization patterns on the membrane lamellarity and, in turn, on the strength of the inhibitory coupling is complemented in Fig. 4 where (a) we combine structural SAXS data (in the insets) and the temporal evolution of observed oscillation periods of four different arrays of diffusively coupled droplets, each characterized by a different dopant in the confining membrane. The 2-period clustering is by far more pronounced in the multilamellar pure

DMPC system, characterized by two marked Bragg's reflection peaks, while it progressively transmutes into a single-period scenario when doping with STS, passing through a period ratio, a, slightly larger than 1 if TA (or Myr-A) are used. With these dopants, Bragg's peaks gradually disappear, indicating a transition from multilamellar to oligolamellar and eventually monolamellar membranes.[30] Figure 4.b gives an overview of the scenarios obtained numerically by tuning the strength of the inhibitory coupling k_W. The occurrence of the period clustering consistent with a synchronization scheme $1{:}a{:}1{:}a$ is transient and confined to a narrow window of k_W values for low k_9, but it can be stabilized by increasing it. This phenomenon appears as an effect of a weak inhibitory coupling among oscillatory drops.

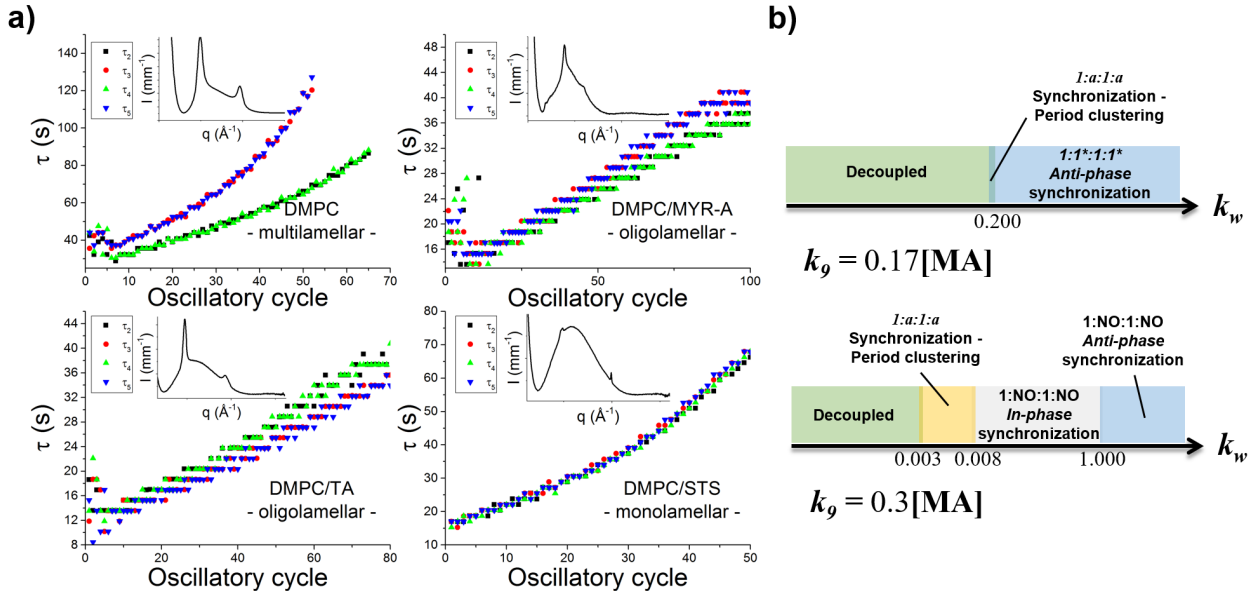

Figure 4: a) Experimental observation of oscillation periods of four communicating droplets in DMPC (upper left panel), DMPC/Myr-A (upper right panel), DMPC/TA (lower left panel) and DMPC/STS (lower right panel) droplets. The behaviour of the oscillation periods was found to change according to the membrane lamellarity, indicated by the SAXS data in the insets.[30] Note that experimental timeseries are not stationary and the period grows as the the main reactants are depleted. b) Parameter diagram of the synchronisation scenarios obtained numerically by varying the strength of the inhibitory coupling, k_W, for two different values of k_9 ($k_X \leq 0.001$ s^{-1}, $k_s^W = 0$). $1:a:1:a$ indicates alternate synchronization among successive oscillators with a period ratio a; **NO** means "no oscillations".

In conclusion, by changing the physico-chemical properties of the confining membranes with different dopants, the diffusion-driven chemical communication among drops could be

controlled to induce distinct collective behaviours. Some of these were found to be consistent with already known synchronisation patterns obtained in diffusively-coupled and pulsed-coupled networks of oscillators. By contrast, the 1:a:1:a *period-locking* regimes obtained when emulsions are separated by a multilamellar membrane, represents a novel scenario in this panorama. A simple kinetic framework based on the classic Oregonator model gives a unifying picture and understanding of the dynamics observed experimentally and suggests new synchronisation patterns that can be obtained with this biomimetic model system.

Acknowledgement

Thanks are due to the ESRF (Grenoble) for granting time allocation at the ID02 beamline where the SAXS diagrams were recorded. M.A.B. gratefully acknowledges funding by F.R.S.-FNRS and from Programma Operativo Nazionale (PON) Ricerca e Innovazione 2014–2020, Asse I "Capitale Umano", Azione I.2 A.I.M. "Attrazione e mobilitá dei ricercatori", Linea 2 (Attrazione dei Ricercatori). K. T and A. AH acknowledge funding from the Doctoral School ED398 Chimie Physique et Chimie Analytique de Paris Centre.

Supporting Information Available

The following files are available free of charge.

- budroni_SI.pdf: experimental and numerical details.

References

(1) Berg, H. C. Random Walks in Biology; Princeton University Press, 1993.

(2) Farsad, N.; Yilmaz, H. B.; Eckford, A.; Chae, C.; Guo, W. A Comprehensive Survey

of Recent Advancements in Molecular Communication. IEEE Communications Surveys Tutorials **2016**, 18, 1887–1919.

(3) Nakano, T.; Eckford, A. W.; Haraguchi, T. Molecular Communication; Cambridge University Press, 2013.

(4) Krauss, G.; Schönbrunner, N.; Cooper, J. Biochemistry of signal transduction and regulation; Wiley Online Library, 2003; Vol. 3.

(5) Papin, J. A.; Hunter, T.; Palsson, B. O.; Subramaniam, S. Reconstruction of cellular signalling networks and analysis of their properties. Nat. Rev. Mol. Cell Biol. **2005**, 6, 99–111.

(6) Berridge, M. J. The AM and FM of calcium signalling. Nature **1997**, 386, 759–760.

(7) Taylor, A. F.; Tinsley, M. R.; Wang, F.; Huang, Z.; Showalter, K. Dynamical Quorum Sensing and Synchronization in Large Populations of Chemical Oscillators. Science **2009**, 323, 614 –617.

(8) Horvath, V.; Gentili, P. L.; Vanag, V. K.; Epstein, I. R. Pulse-Coupled Chemical Oscillators with Time Delay. Angew. Chem., Int. Ed. **2012**, 51, 6878–6881.

(9) Totz, J. F.; Rode, J.; Tinsley, M. R.; Showalter, K.; Engel, H. Spiral wave chimera states in large populations of coupled chemical oscillators. Nat. Phys. **2018**, 14, 282–285.

(10) Vanag, V. K. "Cognitive" modes in small networks of almost identical chemical oscillators with pulsatile inhibitory coupling. Chaos **2019**, 29, 033106.

(11) Grecco, H.; Schmick, M.; Bastiaens, P. H. Signaling from the Living Plasma Membrane. Cell **2011**, 144, 897–909.

(12) Belousov, B. P. A periodic reaction and its mechanism. Sbornik Referatov po Radiatsonno Meditsine. Moscow, 1958; pp 145–147.

(13) Zhabotinsky, A. M. Periodic liquid phase reactions. Proc. Acad. Sci. USSR **1964**, 157, 392–395.

(14) Toiya, M.; Vanag, V. K.; Epstein, I. R. Diffusively Coupled Chemical Oscillators in a Microfluidic Assembly. Angew. Chem., Int. Ed. **2008**, 47, 7753–7755.

(15) Torbensen, K.; Rossi, F.; Ristori, S.; Abou-Hassan, A. Chemical communication and dynamics of droplet emulsions in networks of Belousov-Zhabotinsky micro-oscillators produced by microfluidics. Lab. Chip **2017**, 17, 1179–1189.

(16) Rossi, F.; Torbensen, K.; Ristori, S.; Abou-Hassan, A. Artificial Life and Evolutionary Computation; Communications in Computer and Information Science; Springer, Cham, 2018; Vol. 830; pp 16–31.

(17) Delgado, J.; Li, N.; Leda, M.; González-Ochoa, H. O.; Fraden, S.; Epstein, I. R. Coupled oscillations in a 1D emulsion of Belousov–Zhabotinsky droplets. Soft Matter **2011**, 7, 3155.

(18) Litschel, T.; M. Norton, M.; Tserunyan, V.; Fraden, S. Engineering reaction–diffusion networks with properties of neural tissue. Lab. Chip **2018**, 18, 714–722.

(19) Toiya, M.; González-Ochoa, H. O.; Vanag, V. K.; Fraden, S.; Epstein, I. R. Synchronization of Chemical Micro-oscillators. J. Phys. Chem. Lett. **2010**, 1, 1241–1246.

(20) Tompkins, N.; Cambria, M. C.; Wang, A. L.; Heymann, M.; Fraden, S. Creation and perturbation of planar networks of chemical oscillators. Chaos **2015**, 25, 064611.

(21) Norton, M. M.; Tompkins, N.; Blanc, B.; Cambria, M. C.; Held, J.; Fraden, S. Dynamics of Reaction-Diffusion Oscillators in Star and other Networks with Cyclic Symmetries Exhibiting Multiple Clusters. Phys. Rev. Lett. **2019**, 123, 148301.

(22) Tompkins, N.; Li, N.; Girabawe, C.; Heymann, M.; Ermentrout, G. B.; Epstein, I. R.;

Fraden, S. Testing Turing's theory of morphogenesis in chemical cells. Proc. Natl. Acad. Sci. USA **2014**, 111, 4397–4402.

(23) Turing, A. M. The Chemical Basis of Morphogenesis. Philos. Trans. R. Soc. Lond. B. Biol. Sci. **1952**, 237, 37–72.

(24) Kondo, S.; Miura, T. Reaction-diffusion model as a framework for understanding biological pattern formation. Science **2010**, 329, 1616–1620.

(25) Bullara, D.; De Decker, Y. Pigment cell movement is not required for generation of Turing patterns in zebrafish skin. Nat. Comm. **2015**, 6, 6971.

(26) Tomasi, R.; Noel, J.-M.; Zenati, A.; Ristori, S.; Rossi, F.; Cabuil, V.; Kanoufi, F.; Abou-Hassan, A. Chemical communication between liposomes encapsulating a chemical oscillatory reaction. Chem. Sci. **2014**, 5, 1854–1859.

(27) Torbensen, K.; Ristori, S.; Rossi, F.; Abou-Hassan, A. Tuning the Chemical Communication of Oscillating Microdroplets by Means of Membrane Composition. J. Phys. Chem. C **2017**, 121, 13256–13264.

(28) Rossi, F.; Zenati, A.; Ristori, S.; Noel, J.-M.; Cabuil, V.; Kanoufi, F.; Abou-Hassan, A. Activatory Coupling Among Oscillating Droplets Produced in Microfluidic Based Devices. Int. J. Unconv. Comput. **2015**, 11, 23–36.

(29) Aufinger, L.; Simmel, F. C. Establishing Communication Between Artificial Cells. Chem-Eur. J. **2019**, 25, 12659–12670.

(30) Torbensen, K.; Rossi, F.; Pantani, O. L.; Ristori, S.; Abou-Hassan, A. Interaction of the Belousov–Zhabotinsky Reaction with Phospholipid Engineered Membranes. J. Phys. Chem. B **2015**, 119, 10224–10230.

(31) Di Cola, E.; Torbensen, K.; Clemente, I.; Rossi, F.; Ristori, S.; Abou-Hassan, A. Lipid

stabilized Water- Oil Interfaces Studied by Micro Focusing Small Angle X-ray Scattering. Langmuir **2017**, 33, 9100–9105.

(32) Field, R. J.; Koros, E.; Noyes, R. M. Oscillations in chemical systems. II. Thorough analysis of temporal oscillation in the bromate-cerium-malonic acid system. J. Am. Chem. Soc. **1972**, 94, 8649–8664.

(33) Budroni, M. A.; Rossi, F. A Novel Mechanism for in Situ Nucleation of Spirals Controlled by the Interplay between Phase Fronts and Reaction–Diffusion Waves in an Oscillatory Medium. J. Phys. Chem. C **2015**, 119, 9411–9417.

(34) Vanag, V. K.; Epstein, I. R. A model for jumping and bubble waves in the Belousov-Zhabotinsky-aerosol OT system. J. Chem. Phys. **2009**, 131, 104512–7.

(35) Scott, S. K. Chemical Chaos; Oxford University Press: Oxford, UK, 1993.

(36) Li, N.; Delgado, J.; González-Ochoa, H. O.; Epstein, I. R.; Fraden, S. Combined excitatory and inhibitory coupling in a 1-D array of Belousov-Zhabotinsky droplets. Phys. Chem. Chem. Phys. **2014**, 16, 10965–10978.

(37) Proskurkin, I. S.; Vanag, V. K. Dynamics of a 1D array of inhibitory coupled chemical oscillators in microdroplets with global negative feedback. Phys. Chem. Chem. Phys. **2018**, 20, 16126–16137.